Engineering Solid Mechanics 11 (2023) 401-410

Contents lists available at GrowingScience

Engineering Solid Mechanics

homepage: www.GrowingScience.com/esm

Numerical analysis of mixed-mode I+II fracture behavior of automotive PVB laminated glass using a novel beam-type test specimen

Alireza Ashkpour[a], Jamal Bidadi[a] and Hamed Saeidi Googarchin[a*]

[a]*Automotive Fluids and Structures Analysis Research Laboratory, School of Automotive Engineering, Iran University of Science & Technology, Tehran, Iran*

ARTICLE INFO

Article history:
Received 10 April 2023
Accepted 16 May 2023
Available online
16 May 2023

Keywords:
Laminated Glass (LG)
Fracture Energy
Mixed-Mode I/II
Stress Intensity Factor
Four-Point Bend

ABSTRACT

Laminated glass is a composite structure consisting of a polymeric interlayer (e.g., polyvinyl butyral PVB) sandwiched between two glass plies. Due to the increasing use of laminated glass (LG) in advanced industries such as automotive sectors, it is of much importance to investigate the fracture behavior of such structures. One of the most critical steps in outlining the fracture behavior of laminated glass is the accurate determination of the fracture energy of the interlayer, usually, polyvinyl butyral (PVB), which is obtained from experimental methods. So far, various laboratory samples have been presented to measure the fracture energy of laminated glass, each of which has its advantages and limitations. In this paper, a new loading setup is proposed for the determination of mixed-mode I/II fracture energy in a rectangular-shape laboratory sample of laminated glass. The loading setup consists of a rectangular beam under a four-point bending which has been analyzed by the commercial ABAQUS software package. By utilizing this specimen, the fracture energy of the combined modes from pure mode I to pure mode II in the PVB interlayer can be measured. The proposed geometry here is simpler than other available geometries in the literature and also it does not require a complex loading mechanism. The effects of crack length ratio and also the support distance on fracture parameters such as and are well investigated.

1. Introduction

Recently, laminated glass has been paid more and more attention in many advanced industrial applications, especially in the automotive, architectural, and aerospace sectors. This is mainly because the lamination of glass with the high-performance polymeric interlayers such as plasticized polyvinyl butyral (PVB), SentryGlas® (SG), and ionoplast interlayer facilitates capability of glass products in structural applications. For example, as a front windshield of an automobile, PVB layer can dissipate the energy during head impact of both passengers and pedestrians to windshield, preventing the accentuation of impact force in a small area, and reducing the head injury. Moreover, PVB keeps the sharp shards of cracked glass together, not allowing them to shatter toward the passengers. Apart from injury reduction, it can also be used in bullet proof glasses as a protection for critical places such as banks and jewelry stores. Due to far less magnitude of the PVB shear modulus compared to that of the glass, its great optical and adhesion features, it is considered as the most frequently used interlayer in industry.

Notable models have been produced in order to extract and anticipate the mechanical fracture properties (Akbardoost & Bidadi, 2020; Aliha et al., 2021; Arora et al., 2018; Bidadi et al., 2023; Choubey & Kumar, 2022; Choupani & Torun, 2022; Mirsayar, 2013, 2014, 2017), breakage (Barrinaya et al., 2022; Khansari et al., 2019) and post-breakage behaviors of different materials in mixed mode (Aliha et al., 2016, 2013; Ayatollahi et al., 2011; Ayatollahi & Aliha, 2007, 2009, 2011; Bidadi et al., 2023; Bidadi et al., 2020, 2022, 2023; Emri & Knauss, 1995; Malek & Keymanesh, 2023; Ragab & Bayoumi, 2018; Shahbazian & Mirsayar, 2023) including laminated composites and specifically laminated glass. In most of the proposed

* Corresponding author.
E-mail addresses: hsaeidi@iust.ac.ir (H. Saeidi Googarchin)

ISSN 2291-8752 (Online) - ISSN 2291-8744 (Print)

doi: 10.5267/j.esm.2023.5.004

models, delamination of the PVB layer from the glass is of the greatest importance. In fact, adhesion of the glass shards to the PVB layer after the failure is highly dependent on the interfacial properties between glass and PVB. Fracture mechanics is a branch of solid mechanics which evaluates the onset and propagation of crack in structures while holding the premise of the existence of an initial defect such as a crack in material.

In order to evaluate the different loading conditions in structures, stress field, and the displacements on the edge of the crack are divided into three categories, according to the type of the crack faces differentiation toward each other: Mode I, in which the crack surfaces tend to open apart from each other. In mode II and III, the slipping occurs between the crack surfaces that in mode II it is perpendicular to the crack plane and parallel with crack front, and finally, in mode III the slipping is parallel with both crack front and crack surfaces.

Moreover, this is an approach for anticipating the fracture load of structural joints such as PVB adhesion in laminated glass. In fracture mechanics two criteria are studied:

1) Criterion based on stress intensity factors: In this criterion, stress intensity factors are utilized as the design parameter. This factor depends on the specimen geometry, crack length, and the stress distribution. Based on this criterion, a crack propagates when the stress intensity factor at the crack tip attains its critical value which is called fracture toughness.

2) Criterion based on the fracture energy: In this criterion, the crack propagates when the rate of energy-releasing reaches the critical value (i.e., Fracture energy) which is an inherent property.

In order to carry out the numerical simulation, interfacial fracture properties of laminated glass layers are required. Due to the possibility of the unanticipated damages to glass, obtaining mentioned properties is a challenging work. A few experimental methods have been developed toward this end in the past, including the through-cracked tensile (TCT) (Amin et al., 2019) test and compressive shear test (CST) (Chen et al., 2021; Jagota et al., 2000). The TCT test employs cracked glass plies bridged by the PVB interlayer under tension, while the CST involves loading a glass laminate in compression and shear at a specified angle to the loading direction (Poblete et al., 2022). Recently, a modified Arcan test was introduced in order to evaluate Mode II fracture toughness of a laminated glass specimen. It is shown that despite its complex configuration, it is able to yield precise results. However, all types of tests mentioned above can yield fracture toughness in only pure mode II. So, in order to evaluate the fracture properties of Mode I and mixed-Mode I/II, it is needed to utilize other test methods. Double-Cantilever Beam (DCB) test, due to its simplicity, is considered as one of the popular tests, and is employed to extract fracture properties of laminated glass in Mode I, and Peel test is also used for extracting mixed-Mode fracture properties (Poblete et al., 2022). As is illustrated in Fig. 1, peel test needs a specific form of specimen and traditional two-ply laminated glass is of no usage. Actually, it uses a single glass ply with a PVB layer perpendicular to the lower glass layer.

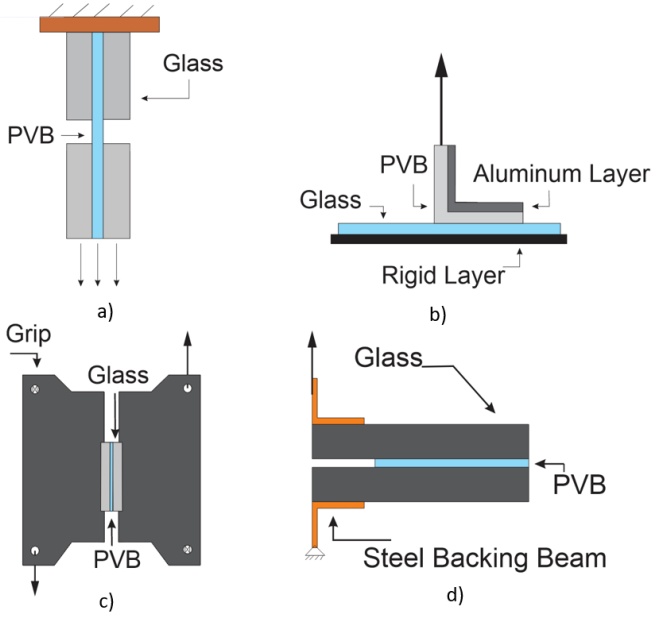

Fig. 1. Different test specimens in references in for evaluating fracture energy of laminated glass a) TCT test, b) Peel test, c) Modified Arcan test, d) DCB test

In this study, the goal is to introduce a simple four- point bend test specimen which does not need the complexity and limitations of the prior specimens. In addition, it should be capable of producing pure mode I and II along with mixed mode

I/II, only by changing the location of support and loading points. It consists of two frame-type grips and a laminated glass specimen is located middle of them which connects the two mentioned parts.

2. Material and Method

In this study, the goal is to introduce a simple four- point bend test specimen which does not need the complexity and limitations of the prior specimens. In addition, it should be capable of producing pure mode I and II along with mixed mode I/II, only by changing the location of support and loading points. It consists of two frame-type grips and a laminated glass specimen is located in the middle

The aim of this paper is to introduce and numerically analyze a test specimen which would make it possible to compute the fracture energy of PVB layer in the mixed mode I/II.

This geometry is made up of two rectangular-section beams each of which are separately connected to the glass specimen using an adhesive layer. As is illustrated in Fig. 2 the overall length of the system is shown as L and specimen's height is W. A crack is also located at the layer connecting the PVB to glass with a length of *a*. When the specimen undergoes symmetric bending, pure mode I is generated and the same happens for mode II when an asymmetric bending load is exerted. In configuration of mode I, the distance between the loading points is called $2S_2$ and the corresponding distance between the supports is also $2S_1$. The mentioned distance in pure mode II and mixed mode I/II would be S_1+S_2. In order to generate the mixed-mode I/II in this specimen S_1 parameter is changed in mode I and II. In mode I $S_1>S_2$ at the initial condition, and decreasing S_1 toward S_2 could generate mixed mode I/II. Fig. 3 depicts the asymmetric loading condition and relocating of the system to produce mixed mode I/II in accordance with shear force and bending moment diagrams.

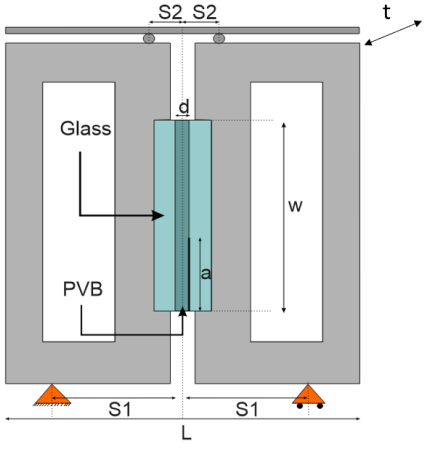

Fig. 2. The schematic of symmetrical loading configuration (Pure Mode I).

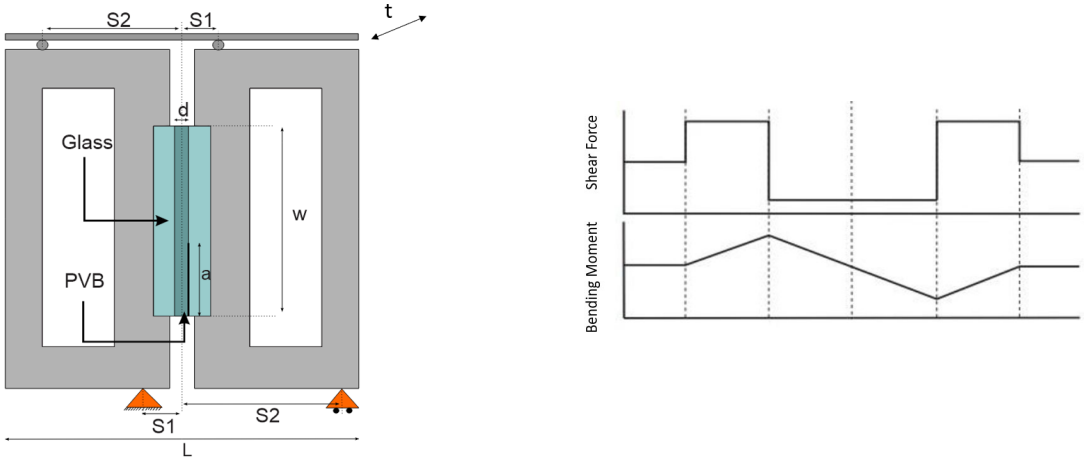

Fig. 3. The schematic of asymmetrical loading configuration (Pure Mode II).

Implementing experimental studies is always concomitant with limitations such as time and economic factors and possible errors in the process of experiments and measurements. Since, implementing numerical methods along with experimental studies could be a useful way of evaluating such structures.

Finite Element Method (FEM) is considered among the most efficient numerical methods in engineering sciences. FEM could be utilized to solve issues containing discontinuities such as crack, in the area of fracture mechanics. Implementing this method for evaluating different issues has contributed to emergence and improvement of software and strong solvers, and ABAQUS commercial software is surely one of the most powerful ones. In this study, a 3D model is implemented and evaluated in order to enhance the precision of the results. In addition, due to the complexities and uncertainties of analytical solution due to the non-linear behavior of the materials, the behavior of PVB layer is considered linear elastic.

FEM analysis of the specimen is conducted in the ABAQUS software with the assumption of 3D model and linear elastic behavior (LFEM). In Table 1 the mechanical characteristics of the PVB and glass are shown.

In this specimen, a laminated glass with two glass layers with 10 mm thickness is implemented. A crack with a length of *a* is modeled as a plane along the PVB layer with Contour-Integral method. Direction of the crack propagation is also considered to be in parallel with the initial crack. An arbitrary force of *P* is determined 5000 N and is exerted as is shown in Fig. 3. In order to create the supporting condition a roller support in which the specimen is fixed in the y direction, and another one which is a simple support that fixes the specimen in both x and y direction are implemented. While meshing, after evaluating the independence of the mesh, a number of 20808 elements are used. To enhance the precision of the results at the vicinity of the crack, singular elements are chosen for this region. Meshing of the component, initial crack, load and support points in mode II are illustrated in Fig. 4. Like Fig. 4 the density of the elements is higher at the vicinity of the crack compared to the other regions.

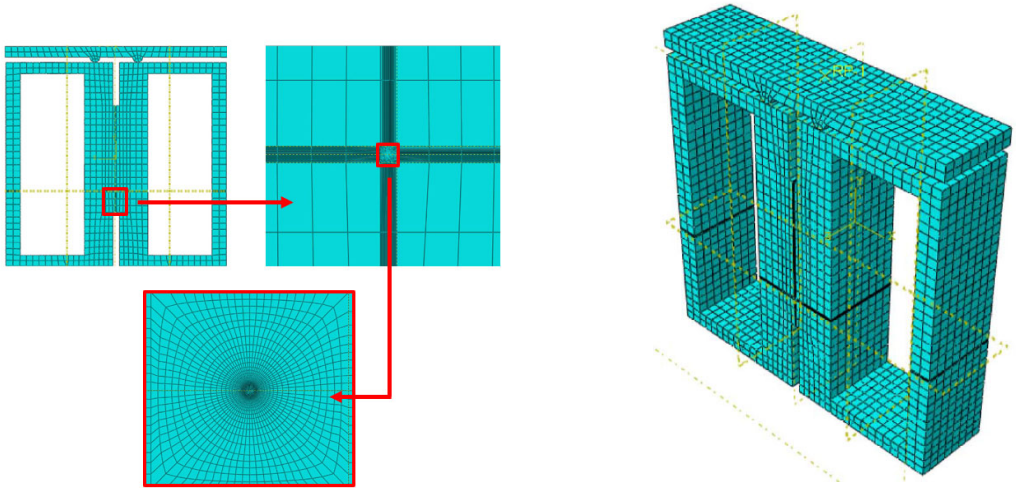

Fig. 4. Finite Element Mesh Model

Table 1. Mechanical Characteristic of the used materials

Material	Young Modules (MPa)	Poisson Ratio
PVB	700	0.36
Glass	5×10^3	0.28
Steel	210×10^4	0.31

Desired dimensions of the specimen are achieved so that the angle of the mixed mode undergoes the minimum change relative to crack propagation. Hence, overall height, length and thickness of the apparatus are 190 mm, 206.16 mm, and 50 mm, respectively. Thickness of the PVB layer is also 0.76 mm.

For obtaining pure mode I, the loading condition must be symmetric. Values for S_1 and S_2 should be determined for both mode I and mode II so that the minimum value of K_{II} and K_I is obtained, respectively. Analysis is conducted for 6 different ratios of the crack length to the width of the specimen (a/W) which are 0.2, 0.3, 0.4,0.5,0.6, and 0.7.

Loading and support points, together with geometrical features of the structure are gathered in Table 2. Five loading cases are provided which among them three cases depict mixed-mode I/II and two other cases relate to pure mode I and II.

Stress intensity factors K_I and K_{II} are dependent on the geometry of the specimen and magnitude of loading exerted on it. Therefore, variation of the crack length and loading distances would alter their value. With utilizing ABAQUS and substituting required parameters into the Eq. (1) and Eq. (2), dimensionless geometrical factors of Y_I and Y_{II} could be obtained. Eq. (1) and Eq. (3), are utilized for obtaining geometrical coefficients of the specimen for pure mode I and Eq. (2) and Eq. (4) are for pure mode II:

For mode I:

$$\sigma = \frac{6(S1 - S2)}{tw^2} P \tag{1}$$

For mode II:

$$\sigma = \frac{6(2S1 - S2)}{tw^2} P$$

$$\tau = \frac{3(S2 - S1)}{(tw)(S2 + S1)} \tag{2}$$

Stress Intensity factors:

$$K_{\mathrm{I}} = \sigma\sqrt{\pi a}\, Y_{\mathrm{I}} \tag{3}$$

$$K_{\mathrm{II}} = \sigma\sqrt{\pi a}\, Y_{\mathrm{II}} \tag{4}$$

The angle of mixed mode loading, phase angle, is also defined as Eq. (5):

$$\varphi = tan^{-1}(\frac{K_{II}}{K_I}) \tag{5}$$

When the phase angle is 0 and $\frac{\pi}{2}$, pure mode I and pure mode II is generated, respectively.

Table 2. The values of FE model dimensions

MODE	S1(mm)		S2(mm)		S0(mm)	F(N)	t (mm)
Mode-I	50		20		0.38	5×10^3	50
Mixed-Mode (Fig. 2 adjustment)	80	40	20	20	0.38	5×10^3	50
	60	50	30	20			
	75	30	30	20			
Mode-II	40		90		0.38	5×10^3	50

Finally, by employing Griffits procedure (Griffits, 1995), fracture energy of the interface can be computed after extracting the stress intensity factors from ABAQUS by using Eq. (6):

$$G = \frac{Kc}{E^*} \tag{6}$$

where $\boldsymbol{E^*}$ is the equivalent Young Modulus and can be computed from Eq. (7) (Chen et al., 2022):

$$E^* = \frac{\sigma}{\varepsilon} = \frac{F_u/bt}{\delta/a} \tag{7}$$

where b and t are the width of specimen and nominal thickness of PVB interlayer, respectively. $\boldsymbol{F_u}$ is the peak force, $\boldsymbol{\delta}$ and $\boldsymbol{a}$ are displacement and delamination length at the maximum force.

3. Results and Discussion

Stress intensity factors and dimensionless geometrical factors obtained from Eq. (3) and Eq. (4) for pure mode I and II are provided in Table 3. It can be seen from Fig. 5 & Fig. 6 that the dimensionless geometry factors in both cases, at first, see a sharp decreasing trend and then come to a minimum point with a gradual slope. The same trend could be seen in similar single-edge notched bending specimens previously used. (Ferreira et al., 2021; Fuchs et al., 1981) This phenomenon can be explained by pointing out the stress distribution in the beam. The maximum value of resultant stress due to the bending moment occurs at the bottom of the beam. Hence, the stress at the crack tip will be maximum at the bottom, when the length of crack is at its smallest value, but gradually decreases by enlarging the length of crack along the width (W) of the beam. And because the neutral axis in our specimen is much closer to the top, we face a longer and gradual decreasing region in geometry factor. As is shown in Fig. 6, geometry factor reaches its minimum when a/W=0.7 in pure mode I, and then it starts

to slightly increase. On the other hand, in pure mode II it happens when a/W=0.6 and the increase in geometry factor is more significant.

Table 3. Pure modes I and II Stress intensity factors and related normalized forms (i.e. Y_I and Y_{II})

Mode	a/W	K_I	K_{II}	Y_I	Y_{II}
Pure mode I	0.2	3.15	-	0.2359	-
	0.3	3.10	-	0.1858	-
	0.4	3.19	-	0.1578	-
	0.5	3.15	-	0.1395	-
	0.6	3.1	-	0.1256	-
	0.7	3.15	-	0.1182	-
Pure mode II	0.2	-	2.25	-	0.1577
	0.3	-	2.41	-	0.1379
	0.4	-	2.6	-	0.1289
	0.5	-	2.86	-	0.1268
	0.6	-	3.1	-	0.1254
	0.7	-	3.6	-	0.1255

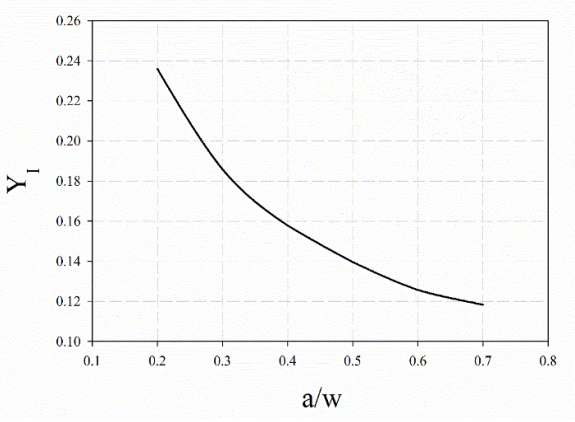

Fig. 5. The normalized stress intensity factor (pure mode I) versus crack length for a constant $S_1/W=0.5$ and $S_2/W=0.2$

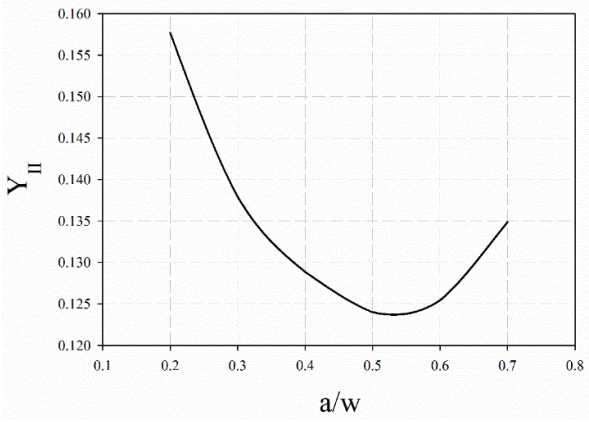

Fig. 6. The normalized stress intensity factor (pure mode II) versus crack length for a constant $S_1/W=0.9$ and $S_2/W=0.4$

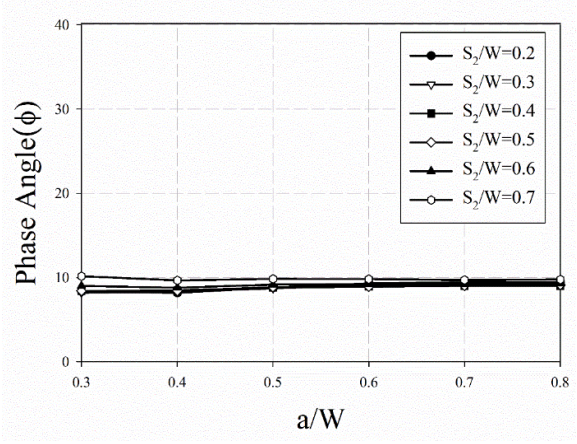

Fig. 7. Phase angle versus a/W for different ratios of S_2/W

Consider the mode I loading adjustment in Fig. 2. Also, by taking into account the definition of phase angle which is defined in Eq. (5), as Fig. 7 shows, the mentioned parameter's variation with crack length. Obviously, phase angle not only does not change with the crack length, but also remains rather steady in 6 different support locations based on Fig. 2 adjustment.

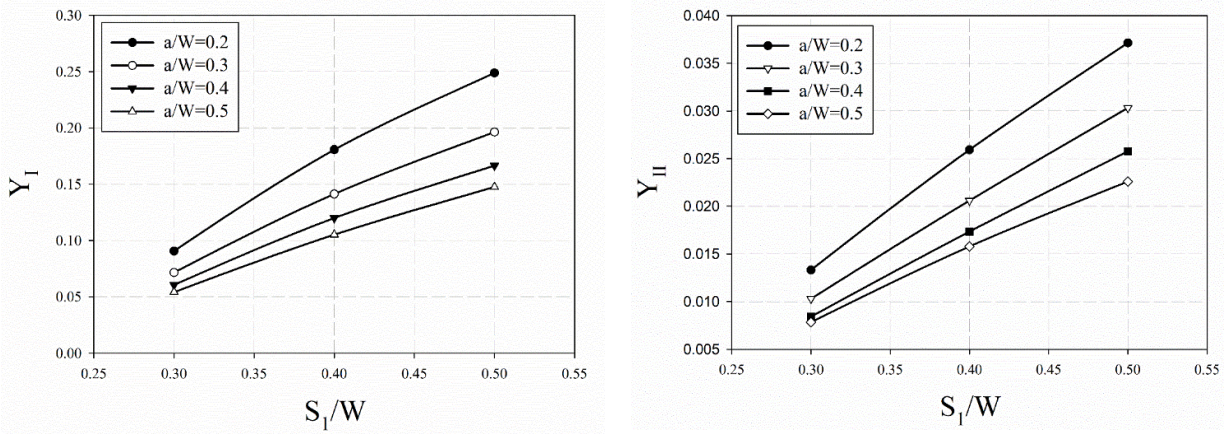

(a) (b)

Fig. 8. Normalized a) mode I and b) mode II stress intensity factor (i.e., Y_I and Y_{II}) for mixed Mode loading based on Fig. 2 adjustment

It is also clear from Fig. 8 that as the distances of two loading points from the center decrease, the contribution of mode I tends to increase. Also, because of the maximum bending moment occurring at the outer edge of the beam, as we increase the crack length, the stress at the tip of the crack decreases gradually. As a consequence, as is depicted in Fig. 8 and Fig. 9, the geometry factor sees the same trend. Dimensionless geometry factors for mixed-mode loading based on Fig. 2 and Fig. 3 adjustment are depicted in Fig. 8 and Fig. 9, respectively. For the first case, S_2 is considered a fixed magnitude of 20mm, where in the second case S_1 is equal to 15mm for every mixed-mode loading case.

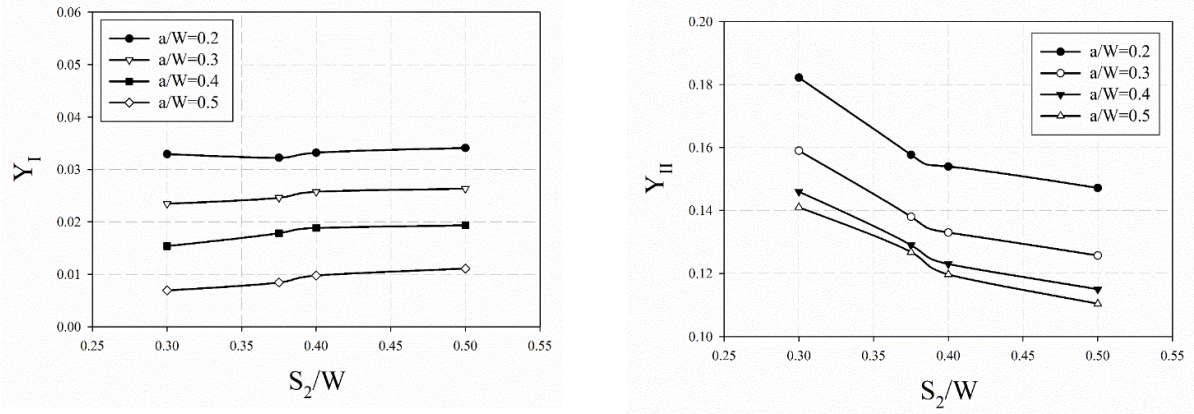

(a) (b)

Fig. 9. Normalized a) mode I and b) mode II stress intensity factor (i.e., Y_I and Y_{II}) for mixed Mode loading based on Fig. 3 adjustment

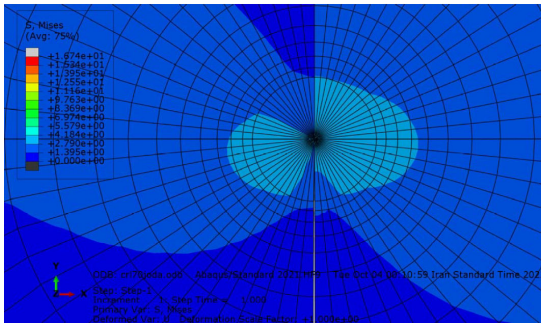

Fig. 10. Stress contour of crack tip under pure mode I

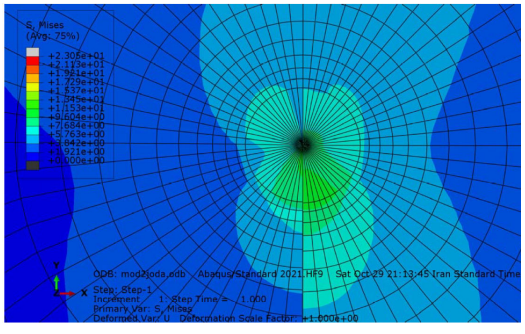

Fig. 11. Stress contour of crack tip under pure mode II

The mises stress contour around the crack tip in pure mode I is depicted in Fig. 10 in which the crack front at the right and left side of the crack is made of glass and PVB, respectively. The value of stress needed to break the glass is about 100 MPa so the glass will remain intact until the end of the experiment. Also, due to the lesser value of PVB's Young Modulus compared with glass, the critical zone in the vicinity of the crack is smaller for PVB than that of glass. The same phenomenon happens in mode II, as is depicted in Fig. 11, in which both the value of mises stress and critical zone is saliently larger for the glass part.

4. Conclusions

Due to the importance of the fracture energy prediction in laminated glass, various specimens with different geometry and loading conditions are designed in order to achieve this aim. In this article, numerical analysis of such a specimen under four-point bending load is conducted to compute the fracture energy in mixed mode I/II. Besides, this specimen possesses a simpler geometry and loading condition and also doesn't need complex fixtures when compared to previous introduced models. With the 3D modeling of this specimen in ABAQUS commercial software for different crack lengths and loading points and supports, stress intensity factors were obtained for this model. The results indicate that this is not only capable of generating pure mode I and pure mode II but also a combination of mode I, and the angle of mixed mode is also independent of the propagation of the initial crack.

References

Akbardoost, J., & Bidadi, J. (2020). Experimental Investigation on the Effect of the Specimen Thickness on the Mode II Fracture Resistance of Rocks. *Journal of Engineering Geology*, *14*(2), 203–222.

Aliha, M. R.M., Bahmani, A., & Akhondi, S. (2016). A novel test specimen for investigating the mixed mode I+III fracture toughness of hot mix asphalt composites - Experimental and theoretical study. *International Journal of Solids and Structures*, *90*, 167–177. https://doi.org/10.1016/j.ijsolstr.2016.03.018

Aliha, M. R.M., Hosseinpour, G. R., & Ayatollahi, M. R. (2013). Application of cracked triangular specimen subjected to three-point bending for investigating fracture behavior of rock materials. *Rock Mechanics and Rock Engineering*, *46*(5), 1023–1034. https://doi.org/10.1007/s00603-012-0325-z

Aliha, Mohammad Reza Mohammad, Kucheki, H. G., & Mirsayar, M. (2021). Mixed mode i/ii fracture analysis of bi-material adhesive bonded joints using a novel short beam specimen. *Applied Sciences (Switzerland)*, *11*(11). https://doi.org/10.3390/app11115232

Amin, M., Cormie, D., Smith, D., Wholey, W., Blackman, B. R. K., Dear, J. P., & Hooper, P. A. (2019). On the bonding between glass and PVB in laminated glass. *Engineering Fracture Mechanics*, *214*(October 2018), 504–519. https://doi.org/10.1016/j.engfracmech.2019.04.006

Arora, P. K., Srivastava, S. C., Lohumi, M. K., & Kumar, H. (2018). Progressive damage response and crack growth direction for multiple through cracks of laminated composite finite plate. *Engineering Solid Mechanics*, *6*(4), 371–389. https://doi.org/10.5267/j.esm.2018.9.003

Ayatollahi, M. R., & Aliha, M. R. M. (2007). Wide range data for crack tip parameters in two disc-type specimens under mixed mode loading. *Computational Materials Science*, *38*(4), 660–670. https://doi.org/10.1016/j.commatsci.2006.04.008

Ayatollahi, M. R., & Aliha, M. R. M. (2009). Analysis of a new specimen for mixed mode fracture tests on brittle materials. *Engineering Fracture Mechanics*, *76*(11), 1563–1573. https://doi.org/10.1016/j.engfracmech.2009.02.016

Ayatollahi, M. R., & Aliha, M. R. M. (2011). On the use of an anti-symmetric four-point bend specimen for mode II fracture experiments. *Fatigue and Fracture of Engineering Materials and Structures*, *34*(11), 898–907. https://doi.org/10.1111/j.1460-2695.2011.01583.x

Ayatollahi, M. R., Aliha, M. R. M., & Saghafi, H. (2011). An improved semi-circular bend specimen for investigating mixed mode brittle fracture. *Engineering Fracture Mechanics*, *78*(1), 110–123. https://doi.org/10.1016/j.engfracmech.2010.10.001

Barrinaya, M. A., Alfiyuranda, M. N., Ramezani, M., Putra, I. S., Ramesh, S., Kadarno, P., Hastuty, S., & Purbolaksono, J. (2022). Modes I-II-III stress intensity factors of a semi-elliptical surface crack at a round bar under torsion loading by FEM and DBEM. *Engineering Solid Mechanics*, *10*(4), 399–406. https://doi.org/10.5267/j.esm.2022.6.099

Bidadi, J., Saeidi Googarchin, H., Akhavan-Safar, A., & da Silva, L. F. M. (2023). Loading rate effects on mixed-mode I/II fracture envelope of epoxy resins with nonlinear behavior. *Theoretical and Applied Fracture Mechanics*, *125*, 103858. https://doi.org/10.1016/j.tafmec.2023.103858

Bidadi, J, Hampaiyan Miandowab1, H., & Saeidi Googarchin, H. (2023). Experimental and Numerical Investigation of the Performance of Automotive Adhesively Bonded Crash Box Beams Under Transverse Loading. *Automotive Science and Engineering*, *13*(2), 4085–4091. https://doi.org/10.22068/ASE.2023.637

Bidadi, Jamal, Akbardoost, J., & Aliha, M. R. M. (2020). Thickness effect on the mode III fracture resistance and fracture path of rock using ENDB specimens. *Fatigue and Fracture of Engineering Materials and Structures*, *43*(2), 277–291. https://doi.org/10.1111/ffe.13121

Bidadi, Jamal, Akbardoost, J., Aliha, M. R. M., Googarchin, H. S., Akhavan-Safar, A., & da Silva, L. F. M. (2023). Mixed-Mode I/II Fracture Load Prediction in Cracked Rock Geometries Using the Tangential Stress Contour (TSC) Method. *1st International Conference on Mechanics of Solids 2022: Selected Contributions of MS 2022*, 65–90.

Bidadi, Jamal, Aliha, M. R. M., & Akbardoost, J. (2022). Development of maximum tangential strain (MTSN) criterion for prediction of mixed-mode I/III brittle fracture. *International Journal of Solids and Structures*, *256*(February), 111979. https://doi.org/10.1016/j.ijsolstr.2022.111979

Chen, S., Chen, Z., Chen, X., & Schneider, J. (2022). Evaluation of the delamination performance of polyvinyl-butyral laminated glass by through-cracked tensile tests. *Construction and Building Materials*, *341*(January), 127914. https://doi.org/10.1016/j.conbuildmat.2022.127914

Chen, X., Rosendahl, P. L., Chen, S., & Schneider, J. (2021). On the delamination of polyvinyl butyral laminated glass: Identification of fracture properties from numerical modelling. *Construction and Building Materials*, *306*(September), 124827. https://doi.org/10.1016/j.conbuildmat.2021.124827

Choubey, R. K., & Kumar, S. (2022). Simplified equations for determining double-k fracture parameters of concrete for compact tension test. *Engineering Solid Mechanics*, *10*(1), 57–70. https://doi.org/10.5267/j.esm.2021.10.002

Choupani, N., & Torun, A. R. (2022). Fracture characterization of bonded composites: A comparative study. *Engineering Solid Mechanics*, *10*(1), 109–116. https://doi.org/10.5267/j.esm.2021.8.001

Emri, I., & Knauss, W. G. (1995). *1st International Conference on Mechanics of Time Dependent Materials*.

Ferreira, D. A., Savioli, R., & Sarzosa, D. F. B. (2021). New formulation for fracture toughness characterization using four-point bend specimens. *Engineering Fracture Mechanics*, *241*(November 2020), 107409. https://doi.org/10.1016/j.engfracmech.2020.107409

Fuchs, H. O., Stephens, R. I., & Saunders, H. (1981). Metal Fatigue in Engineering (1980). In *Journal of Engineering Materials and Technology* (Vol. 103, Issue 4). https://doi.org/10.1115/1.3225026

Griffits, A. A. (1995). The phenomena of rupture and flow in solids. *Masinovedenie*, *C*(1), 9–14. https://doi.org/10.1098/rsta.1921.0006

Jagota, A., Bennison, S. J., & Smith, C. A. (2000). Analysis of a compressive shear test for adhesion between elastomeric polymers and rigid substrates. *International Journal of Fracture*, *104*(2), 105–130. https://doi.org/10.1023/A:1007617102311

Khansari, N. M., Farrokhi, A., & Mosavi, A. (2019). Orthotropic mode II shear test fixture: Iosipesque modification. *Engineering Solid Mechanics*, *7*(2), 93–108. https://doi.org/10.5267/j.esm.2019.4.003

Malek, M., & Keymanesh, M. (2023). Impact of thickness, void content, temperature and loading rate on tensile fracture toughness and work of fracture of asphalt mixtures-An experimental study using the SCB test. *Engineering Solid Mechanics*, *11*(2), 163–174. https://doi.org/10.5267/j.esm.2022.12.004

Mirsayar, M. M. (2013). Calculation of stress intensity factors for an interfacial notch of a bi-material joint using photoelasticity. *Engineering Solid Mechanics*, *1*(4), 149–153. https://doi.org/10.5267/j.esm.2013.09.006

Mirsayar, M. M. (2014). A new mixed mode fracture test specimen covering positive and negative values of T-stress. *Engineering Solid Mechanics*, *2*(2), 67–72. https://doi.org/10.5267/j.esm.2014.2.006

Mirsayar, M. M., Shi, X., & Zollinger, D. G. (2017). Evaluation of interfacial bond strength between Portland cement concrete and asphalt concrete layers using bi-material SCB test specimen. *Engineering Solid Mechanics*, *5*(4), 293–306. https://doi.org/10.5267/j.esm.2017.8.001

Poblete, F. R., Mondal, K., Ma, Y., Dickey, M. D., Genzer, J., & Zhu, Y. (2022). Direct measurement of rate-dependent mode I and mode II traction-separation laws for cohesive zone modeling of laminated glass. *Composite Structures*, *279*(September 2021), 114759. https://doi.org/10.1016/j.compstruct.2021.114759

Ragab, A.-R., & Bayoumi, S. E. (2018). Engineering Solid Mechanics. *Engineering Solid Mechanics*, *11*, 325–338. https://doi.org/10.1201/9780203757307

Shahbazian, B., & Mirsayar, M. M. (2023). Fracture mechanics of cellular structures: past, present, and future directions. *Engineering Solid Mechanics*, *11*(2), 231–242. https://doi.org/10.5267/j.esm.2022.11.004